Article

Wearable Current-Based ECG Monitoring System with Non-Insulated Electrodes for Underwater Application

Stefan Gradl [1],*,† [ID]**, Tobias Cibis [1],†, Jasmine Lauber [1], Robert Richer [1], Ruslan Rybalko [2], Norman Pfeiffer [2], Heike Leutheuser [1], Markus Wirth [1], Vinzenz von Tscharner [3] and Bjoern M. Eskofier [1]** [ID]

[1] Machine Learning and Data Analytics Lab, Department of Computer Science, Friedrich-Alexander-Universität Erlangen-Nürnberg (FAU), Immerwahrstr. 2a, 91058 Erlangen, Germany; tobias.cibis@fau.de (T.C.); laujas@web.de (J.L.); robert.richer@fau.de (R.R.); heike.leutheuser@fau.de (H.L.); markus.wirth@fau.de (M.W.); bjoern.eskofier@fau.de (B.M.E.)

[2] Fraunhofer Institute for Integrated Circuits IIS, Am Wolfsmantel 33, 91058 Erlangen, Germany; ruslan.rybalko@iis.fraunhofer.de (R.R.); norman.pfeiffer@iis.fraunhofer.de (N.P.)

[3] Human Performance Lab, University of Calgary, Calgary, AB T2N 1N4, Canada; tvvon@ucalgary.ca

* Correspondence: stefan.gradl@fau.de; Tel.: +49-9131-8527890

† These authors contributed equally to this work.

Abstract: The second most common cause of diving fatalities is cardiovascular diseases. Monitoring the cardiovascular system in actual underwater conditions is necessary to gain insights into cardiac activity during immersion and to trigger preventive measures. We developed a wearable, current-based electrocardiogram (ECG) device in the eco-system of the FitnessSHIRT platform. It can be used for normal/dry ECG measuring purposes but is specifically designed to allow underwater signal acquisition without having to use insulated electrodes. Our design is based on a transimpedance amplifier circuit including active current feedback. We integrated additional cascaded filter components to counter noise characteristics specific to the immersed condition of such a system. The results of the evaluation show that our design is able to deliver high-quality ECG signals underwater with no interferences or loss of signal quality. To further evaluate the applicability of the system, we performed an applied study with it using 12 healthy subjects to examine whether differences in the heart rate variability exist between sitting and supine positions of the human body immersed in water and outside of it. We saw significant differences, for example, in the RMSSD and SDSD between sitting outside the water (36 ms) and sitting immersed in water (76 ms) and the pNN50 outside the water (6.4%) and immersed in water (18.2%). The power spectral density for the sitting positions in the TP and HF increased significantly during water immersion while the LF/HF decreased significantly. No significant changes were found for the supine position.

Keywords: ECG; immersion; underwater technology

1. Introduction

Cardiovascular diseases constitute the second most common cause of diving fatalities [1]. The Divers Alert Network (DAN) presented in their report some scuba diving fatalities involving U.S. citizens, indicating cardiac diseases as an important factor for those incidents. In many cases, autopsies could not determine people's cause of death. It is assumed that they have died as a result of cardiac dysfunction, because they had manifested coronary artery diseases (CAD). However, the observed lesions have often not been significant enough to warrant an intervention and the deceased had

no reported issues prior to the event. Most of these cases are 'silent' with no prior indication of a problem. It seems that in an immersed condition, minor cardiac dysfunctions may quickly lead to major problems for divers and especially snorkelers [2]. It is known that heart rate variability (HRV) is high at rest and decreases during physical activity [3]. Either a lower than normal HRV under controlled conditions or a reduction in HRV induced by diving would be pathological. It was proposed that a scuba diving candidate showing such characteristics should be further investigated [4]. Therefore, HRV is a highly relevant measure for assessing the autonomous nervous system and has been used for analyzing stress [5], sudden cardiac death [6], or Parkinson's Disease [7].

The pattern of fatality indicates that there is a need for cardiac monitoring while snorkeling or diving in order to predict abnormal cardiac activity during immersion and subsequently activate preventive measures [8]. However, this might not only be important for underwater sports, but also for the monitoring and early detection of heart diseases in elderly [9] during recreational or sporty water activities. It seems plausible that such a monitoring system must be able to correctly assess the HRV as a very important measure of possible heart dysfunction during the transition to a submerged condition. Cardiac activity assessment can be realized using electrocardiography (ECG). There is a wide range of ECG measurement devices for dry conditions, e.g., classical adhesive electrode based solutions, shirts with integrated textile electrodes, handheld devices with metal plate-based electrodes or even chairs with integrated electrodes [9]. Previous studies have also demonstrated the possibility to apply ECG monitoring technology underwater. Schipke [4] performed a study to determine the HRV of divers. Bosco et al. [10] presented a study using a 12-lead Holter monitor to record divers' ECGs. Cibis et al. [11] developed a mobile phone-based ECG, building on the work of Gradl et al. [12], for real-time monitoring of scuba divers. All these systems are based on the concept of potential measurements on the skin surface. However, during immersion in water, this surface potential becomes nearly equipotential due to the high conductivity of water. To allow such ECG systems to still operate underwater, the conventional technologies require adhesive, water-tight sealing of the electrode–skin interface or a complete water-resistant wearable sensor design [13]. Special electrodes employed in underwater potential measurements without adhesive waterproofing were proposed by Othsu et al. [14] and Reyes et al. [15]. While Othsu employed an electrode coated with non-conductive material including a high-input impedance amplifier, Reyes designed an electrode containing two hydrophobic properties, Polydimethylsiloxane (PDMS) and Carbon Black (CB). Pilot studies showed promising correlation of ECGs measured in dry and immersed conditions [16,17]. However, these methods are costly, require an increased manufacturing effort and decrease in performance over exposure time. Furthermore, actual proof of functionality is still missing, since these electrodes were only tested in a bathtub rather than in scuba diving scenarios. It can be assumed that, especially for recreational snorkelers and scuba divers, an easily applicable and cheap solution is required that does not have to rely on additional effort in electrode insulation.

The use of a transimpedance amplifier-based circuit design to enable underwater measurements of biosignals without insulation of the electrodes was successfully demonstrated for the recording of electromyograms [18,19]. In this case, the amplifiers recorded subcutaneous currents elicited by muscles instead of surface potentials. A current amplifier compensates the current arising at the skin surface and thereby actively grounds the area beneath the electrodes. Thus, there are no potential differences between electrodes and no crosstalk. Having both electrodes on ground potential enables the user to perform physiological measurements underwater without electrode insulation because no short circuit will occur.

The use of such a system for ECG measurements was already successfully demonstrated by Omer and Kovacs [20] for normal usage outside of water. They designed, similar to our previous investigation [18,19], a transimpedance amplifier-based circuit with active current feedback and focused on the circuit reliability to reduce baseline drift and amplifier saturation problems. However, they did not evaluate or design the circuit for underwater measurements.

The purpose of this work is therefore to propose an adapted circuit design to be used with submerged electrodes. That circuit is combined with a wearable sensor platform back-end, the FitnessSHIRT (Fraunhofer IIS, Erlangen, Germany) [21]. This allows the system to be accessible in a cheap and very easily applicable manner, even for recreational divers. The performance of the entire system for cardiac monitoring in immersed conditions will be tested by monitoring changes of the HRV between immersed and non-immersed conditions. As stated at the beginning, this is an important characteristic that such a system should be able to assess correctly.

2. Circuit Design

Current practice to measure the cardiac activity is the measurement of potentials arising on the surface of the human body. Hence, the ECG is registered as a potential difference (Φ_1–Φ_2) using two active measurement electrodes. In contrast, the newly designed circuit is based on the assumption that current reflects the cardiac activity equally to the surface potential [19] and therefore intends to amplify current rather than voltage.

An overview of our sensor-system, including the housing, can be seen in Figure 1; the general circuit is illustrated in Figure 2. An ECG signal is registered by a monopolar electrode placed somewhere on the body where electrical currents are induced by the changes in the heart's electrical field. The obtained signal is processed through a transimpedance amplifier and subsequently filtered using a highpass–lowpass configuration. Two filter configurations are implemented and can be selected via a switch. While one filter path provides a wide bandwidth-filtering of 0.5 Hz–1 kHz, the second was implemented with a narrow bandwidth of 7 Hz–24 Hz. This was done in order to have the possibility to measure clinically relevant frequencies (wide) and to also allow a precise and very robust detection of the R-peaks (narrow) [22]. The filtered signal is then amplified using a differential amplifier and converted into a digital signal using an analog to digital (A/D) converter.

(a)　　　　　　　　　　　　　　　　**(b)**
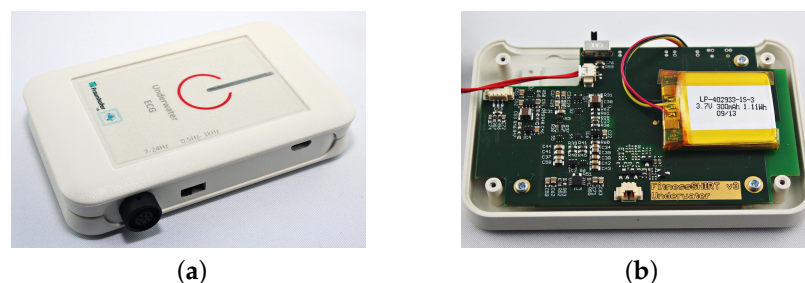
Figure 1. Developed underwater ECG sensor. (**a**) Housing of the sensor. (**b**) Board of the sensor together with the used accumulator.
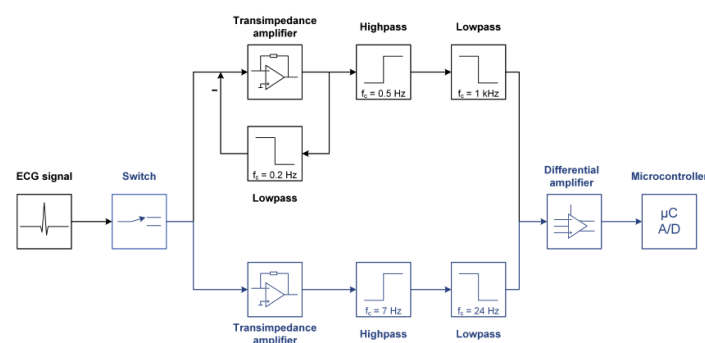

Figure 2. Block diagram of the developed circuit for current-based measurements of the cardiac activity. The circuit was implemented for two bandwidths. In the upper path, the wider range of the bandwidth (0.5 Hz–1 kHz) is illustrated. In the lower path, the small range of the bandwidth (7 Hz–24 Hz) is shown.

2.1. Transimpedance Amplifier

The transimpedance amplifier represents a low ohmic input stage and acts as the central element of the current-based ECG circuit. It translates incoming current into a proportional output voltage. In the proposed circuit, the transimpedance amplifier is designed using a conventional voltage-controlled amplifier where the non-inverting input is connected to a reference electrode; it is thereby actively grounded and the inverting input is connected to the measuring electrode (Figure 3a). The low ohmic input is realized using a virtual shortcut at the input stage of the amplifier. Furthermore, the virtual shortcut provokes both inputs to be on an equal potential $\Phi_+ = \Phi_-$. Due to the low ohmic input of the measuring electrode, the current signal flows into the amplifier and is converted into voltage. A resistance is integrated in the feedback loop, in order to amplify the signal. According to Ohm's and Kirchoff's laws, the output is characterized as:

$$U_{OUT} = -I \times R \tag{1}$$

Besides the signal of interest I_{ECG}, an interfering DC or slow drifting signal I_{noise} can occur and flow over the transimpedance amplifier, causing the amplifier and most likely the following filter stages to overload. Therefore, a feedback loop was implemented to counter the DC and low-frequency drifts by extracting and feeding the interfering signal that was back inverted and processed through a lowpass filter (Figure 3b). This feedback loop is only integrated in the wide frequency range circuit as a low-frequency drift or interfering DC can only occur there.
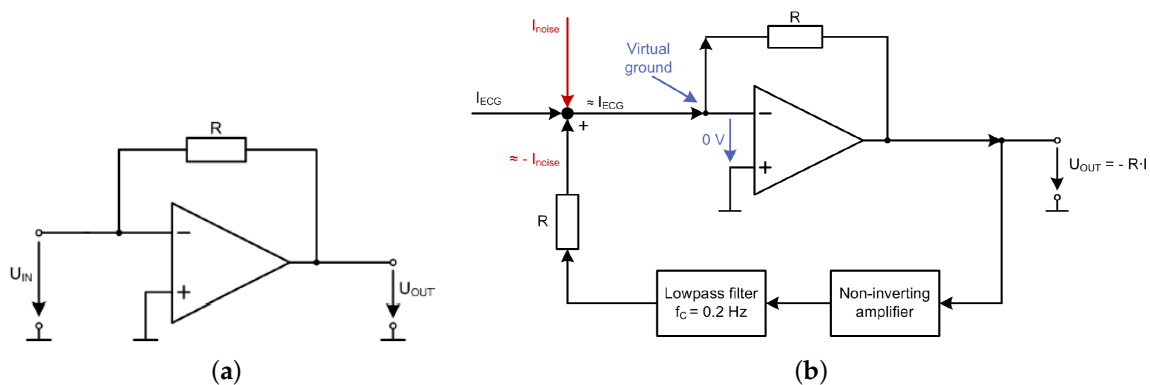
Figure 3. (**a**) Transimpedance amplifier converting the current input signal into a voltage output signal. (**b**) Structural model of the feedback loop to reduce DC/low-frequency interring noises.

2.2. Signal Processing

The obtained voltage output signal from the transimpedance amplifier is further processed by a bandpass filter consisting of a cascaded highpass and lowpass. While the signal in the wide bandwidth range is filtered at the cutoff frequencies $f_c = 0.5\,\text{Hz}$ for the highpass and $f_c = 1\,\text{kHz}$ for the lowpass, the smaller bandwidth range is filtered using the cutoffs $f_c = 7\,\text{Hz}$ and $f_c = 24\,\text{Hz}$, respectively. While the wide bandwidth allows a full representation of the morphology of the cardiac activity to be measured, the smaller bandwidth can be used to extract the QRS complex and to remove noise signal parts for further signal processing. After the bandpass, the filtered signal is further amplified using a differential amplifier and then digitized by the microcontroller, which stores the sampled signal into an internal flash memory. During recording, the signal can also be transmitted wirelessly via Bluetooth to an external device. For all evaluations in this work, we used the signal stored on the internal flash memory which was transferred to a PC after the measurement and then converted and handled in a comma separated values (csv) file.

2.3. Power Supply and Housing

As power supply, a Li-Ion rechargeable battery with an output voltage of 3.7 V, a capacity of 300 mAh and a stored energy of 1.11 Wh is used. The supply voltage is regulated to 3.3 V, as required by some components. A virtual ground point was set at 1.65 V. Hence, the signal swings around this potential. The developed circuit was integrated into a plastic housing for protection. The housing was adapted to the ports and switches of the circuit to enable access (Figure 1). Furthermore, the housing provides a positive effect for the shielding of interferences. A micro USB connector allows the sensor to be charged via USB, and data from the flash memory can be transmitted through this interface. The signal input from the electrodes is realized by an analog cable connector.

3. Physiological Measurements

In addition to a routine electrical evaluation, physiological measurements in dry and immersed conditions were performed using two commercial potential-based ECG sensors and our current ECG. Commercial sensors were the Noraxon Desktop DTS (Noraxon U.S.A., Inc., Scottsdale, AZ, USA) as a Gold-standard reference system for dry measurements and the Shimmer2 (Shimmer Research Ltd., Dublin, Ireland) ECG sensor for underwater measurements. The Shimmer device allowed the attachment of extended electrode cables (up to 1.5 m) allowing comfortable water access. The measurements were performed either with metal-plate electrodes or with Ag/AgCl adhesive foam electrodes. We recorded data from five different adult subjects (two male, three female). All recorded data showed the same characteristics as described in the following. We therefore use one of those datasets, from a healthy male participant, to demonstrate the signals and our findings. We tried several different electrode positions for the measurement electrode (e.g., on the wrist or all typical 12-lead ECG electrode positions). However, most showed similar signal characteristics (Figure 4). In the dry environment, measurements using the wide range configuration showed accurate morphology of the ECG. However, the signal was strongly overlapped with 50 Hz power line interferences (Figures 5(a-II) and 4), however, those can be easily removed using a notch filter in a post-processing stage. This was not done for these figures in order to clearly show the difference between various electrode positions (Figure 4) and the overall impact of noise on the circuit. In contrast, the small range configuration showed very little noise but due to the small bandwidth several morphological ECG events were filtered as well.

Current-based measurements in immersed conditions corresponded to those obtained in dry conditions. The wide bandwidth configuration still showed power line artifacts, however, the signal-to-noise ratio was much higher than outside the water (see Figure 5). One particularly influencing noise characteristic in underwater measurements, which is also visible in Figure 5, is a heavy baseline wandering, which is very rapid and unpredictable. In severe cases, this caused the potential ECG's ADC to go into saturation. While also still visible in the current ECG, it is not as susceptible to those problems. The small bandwidth configuration depicted almost no additive noise. The QRS complex was correctly amplified.

In order to prove the accurate working of the current-based ECG, the sensor was compared to two commercial potential-based ECGs. To compare the current-based sensor, measurements were performed simultaneously using both current and commercial ECG sensors. Figure 5a demonstrates the simultaneous measurement of both sensors. Due to the internal circuit of the commercial sensor, a greater amplitude occurs in comparison to the current-based ECG senor. The measurement displays an accurate reproduction of the ECG signal using the current-based sensor and no mutual influence of both when measured simultaneously. QRS complexes seen in the potential-based ECG sensor correspond to those identifiable in the signal of the newly developed current-based sensor. However, the commercial sensor showed an increase of interferences in immersed condition. The reference potential-based sensor was not able to record an accurate morphologically interpretable ECG.
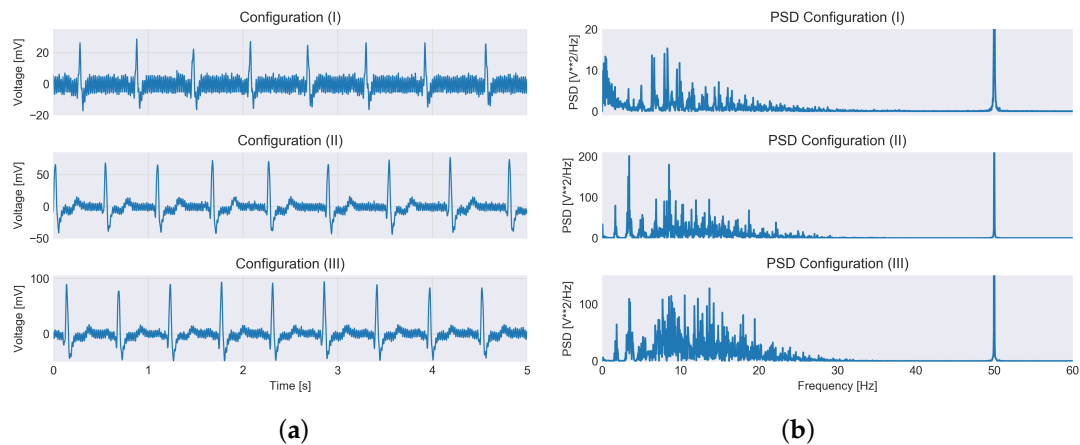
Figure 4. Comparison of measured signal (**a**) and power spectral density (PSD); (**b**) of that signal from our device using different electrode placements. In configuration (I), the measurement electrode was placed on the proximal backside of the right arm wrist. In configuration (II), the measurement electrode was placed on the chest skin at the third intercostal space between the sternum and the midclavicular line. In configuration (III), the measurement electrode was placed on the chest skin at the sixth intercostal space at the midclavicular line. All three configurations show a typical PSD. The heart rate was about 100 beats per minute, thus 1.6 beats per second for case 1 and 3 but was lower for case 2. Thus, peaks can be expected at 1.6 Hz and at the higher order frequencies that are multiples of the 1.6 Hz. This distinct structure gets smeared out when the heart rate variability is large. In case 1, where the signal shows a lower amplitude than when measured at the chest locations, the signal-to-noise ratio is lower and the power of the low-frequency base line fluctuations becomes visible.
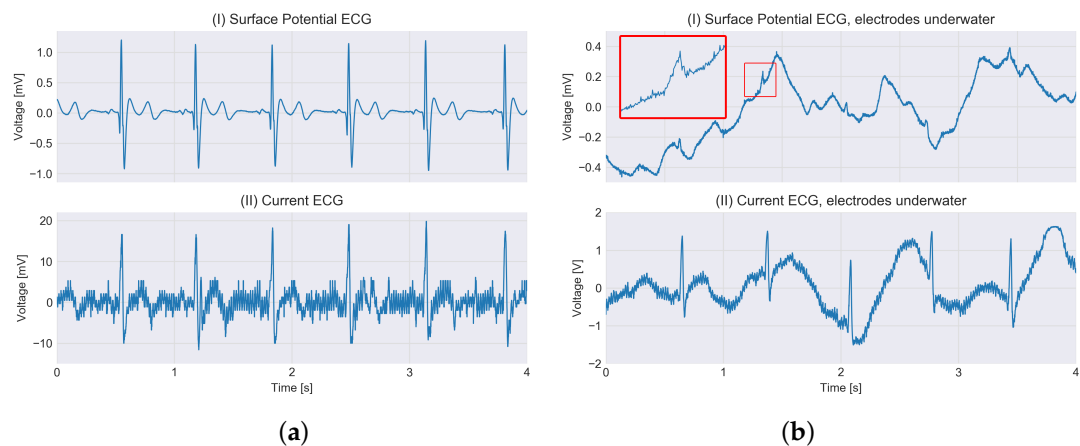
Figure 5. Left side (**a**): Comparison between a commercial surface potential-based ECG (I) and the current-based ECG in the wide bandwidth configuration (II), both showing the same six heartbeats of one healthy person not immersed in water. The potential ECG was filtered in its device while the current-based ECG was not post-filtered, e.g., using a notch filter, at all to allow inspection of the signal behavior around the QRS complex and the influence of the power-line interferences. Measurement electrodes were placed in a lead II configuration. Right side (**b**): Comparison between a commercial surface potential-based ECG (I) and the current-based ECG in the wide bandwidth configuration (II), both showing a 4 s window of the measured ECG with the torso and the attached electrodes fully submerged in water. Both measurements were made with metal-plate electrodes from one healthy person. The QRS complexes of the potential ECG are hardy measurable any more and are severely distorted due to the loss in signal strength. In contrast, the current ECG also shows some baseline wandering, however it is overall much more stable also in the amplitudes of the QRS complexes, which even show an increased signal-to-noise ratio compared to dry conditions.

The demonstrated results show an improvement of the newly developed sensor regarding the signal quality compared to a commercial reference ECG sensor in immersed conditions. Based on the filter design with a bandwidth of 7 Hz–24 Hz, only the QRS complex is extracted. Due to that narrow passband, most of the other parts of the ECG signal beside the QRS complex are lost. In general, the new board shows less influence caused by the powerline. Furthermore, the newly developed sensor was able to record an ECG signal in immersed conditions without loss of signal quality.

Compared to the potential-based sensors, the newly developed board showed advantages regarding the nonexistent low-frequency drift. Furthermore, the signal of the Shimmer sensor was attenuated, likely due to the conductivity of water as already mentioned by Kwatra et al. [23]. Overall, the current-based system proves to be more reliable during recordings under immersed conditions.

4. Heart Rate Variability (HRV) Study

In order to examine the functionality of the developed sensor circuit and its embedding in the FitnessSHIRT platform, we conducted a study to examine the differences in the HRV of humans that have their body almost fully immersed in water (head out immersion [4]) compared to a non-immersed condition. We compare our findings to those made by Schipke and Pelzer [4] to verify that our system is equally suited for such measurements as the one they used, an FDA-cleared, potential-based Holter monitor system with insulated electrodes. As we discussed at the beginning, the HRV changes when submerged in water are a very important indicator for the cardiovascular health and thus an important characteristic that an underwater ECG system should be able to assess. The null hypothesis of our study is therefore that there is no change in HRV parameters between immersed and non-immersed conditions.

4.1. Subjects

We recruited 12 volunteering students, five female and seven male, aged 27 ± 2.8 years (M $\pm$ SD). Their mean height was 1.77 ± 0.07 m and weight 72 ± 11 kg. All participants provided written consent to participate in the study. The average sport workload was 3.1 h per week. To reduce physiological influences on the HRV [24], all subjects were non-smokers, had no cardiovascular problems, no acute diseases and were asked not to consume alcohol or caffeine up to 12 h before the measurements.

4.2. Method

The study was performed in a swimming pool with a water depth of <1 m and stairs. The average water temperature was 30.2 °C with a chlorine content of 0.05 mg/L. The measurements outside the swimming pool were also performed in the same room with an average air temperature of 26.3 °C. All measurements were performed between 1 pm and 4 pm in the afternoon to reduce influences of the circadian rhythm [24] and provide standardized conditions across all subjects.

We recorded the ECG of all subjects using our described current ECG system and repeated the same procedure for each of them. This is described in the following and also shown in the flowchart (Figure 6) and pictures (Figure 7). After preparation of the skin, the subjects sat in a resting position for 5 min outside the water to slow down the heart rate and ensure equal conditions for all subjects. Then, there was a 10-min measurement period in a sitting position outside the water, then 10-min measurement in supine position outside the water. Then, the subjects were immersed in water. We measured the ECG for 10 min in a sitting position inside the water, then 10 min in a supine position. According to [3], a five minute evaluation period is required for HRV measurements. Therefore, we recorded for 10 min and used a centered window of 5 min within this measurement, where the heart rate was most stable, for each evaluation, as was done in previous work [4]. We also recorded an additional 2-min backstroke exercise for five subjects. This was done to verify that measurements could also be taken during a dynamic task performed in water.
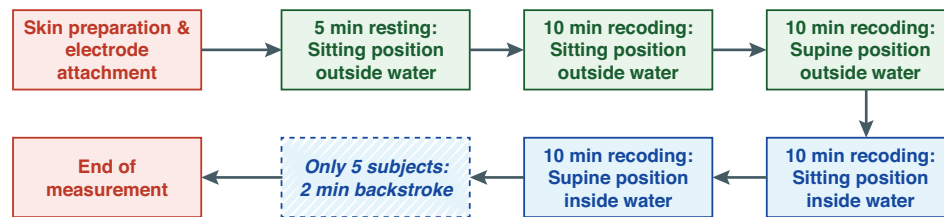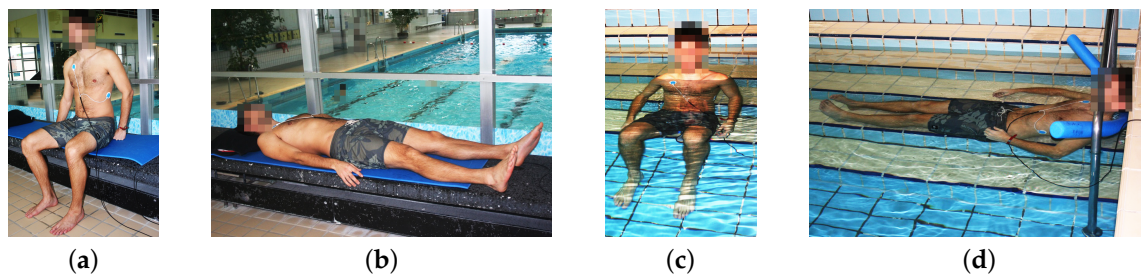
Figure 6. Study procedure for each subject.

| (a) | (b) | (c) | (d) |

Figure 7. Positions of the subjects during the study. (**a**) Sitting position outside water. (**b**) Supine position outside water. (**c**) Sitting position inside water. (**d**) Supine position inside water.

In order to allow a fair comparison to methods using potential-based measurements, e.g., [4], we placed the electrodes in an Einthoven lead II configuration, although, based on the current-circuit's principle, it would be more favorable for the current ECG to have the measurement electrode placed directly above the heart on the left side of the lower sternum.

After the measurement, which was stored on the internal SD-card of the device, the signals were extracted, all R-peaks determined by an automated algorithm [25,26] and manually checked for outliers. All found outliers were corrected manually. The resulting tachogram was equidistantly resampled using a cubic spline interpolation method at a frequency of 6.8 Hz and detrended using a polynomially fitted trend-curve, in order to calculate the spectral power density (PSD) using Fast Fourier Transform with a Hanning window. From the resulting PSD, the frequency parameters were derived.

4.3. Results

We describe the results separated into those obtained from time-domain-based evaluations and afterwards those obtained from frequency-domain-based evaluations. If not stated otherwise, the typical HRV measures are described as proposed or used in previous work [4,24]. In particular, we use the same abbreviations as Schipke and Pelzer [4] to describe specific evaluation parameters of the HRV which are a quasi-standard [27]. We used the Shapiro–Wilk method to test for normal distribution of the data and afterwards the Wilcoxon signed-rank test to obtain the two-sided *p*-value which is given for each statistically significant result in the next two sections. Based on those results, we will be able to reject our null hypothesis.

4.3.1. Time Domain Parameters

Figure 8a shows the results of the evaluated parameters in the time domain, as a mean over all subjects. They are further listed in Table 1. SDNN, RMSSD, SDSD, pNN50 and meanRR showed an increase in the HRV during immersion compared to the positions at the poolside.

(**a**)

(**b**)

(**c**)
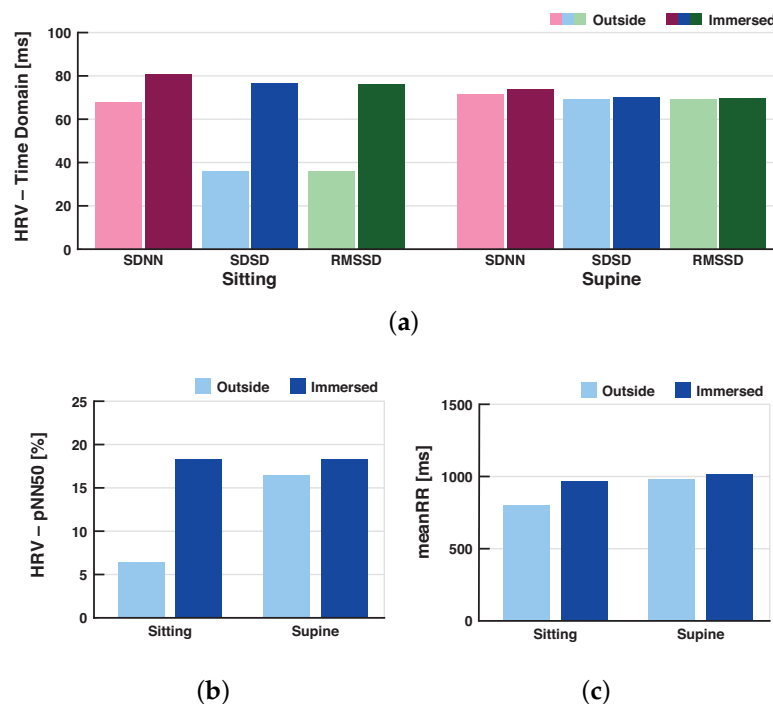
Figure 8. Time domain HRV parameters as a mean over all subjects. Standard deviation of NN intervals (SDNN), standard deviation of successive differences (SDSD) and the root mean square of successive differences (RMSSD) are visualized in (**a**), on the left side for the sitting and on the right side for the supine position. Bright colors are outside the water and dark colors from the immersed condition. In (**b**) the changes in the percentage of the number of adjacent RR intervals which differ more than 50 ms (pNN50) is given and in (**c**) the differences of the arithmetic mean value of all RR intervals.

Table 1. Time domain HRV parameters as a mean over all subjects.

Parameter	Sitting Outside Water	Sitting Inside Water	Supine Outside Water	Supine Inside Water
SDNN [ms]	67.63	80.74 *	71.65	73.80
RMSSD [ms]	36.03	76.33 *	69.13	69.81
SDSD [ms]	36.08	76.46 **	69.24	69.92
pNN50 [%]	6.43	18.24 **	16.43	18.24
meanRR [ms]	801	969 **	977	1017

RMSSD = root mean square of successive differences. **SDSD** = standard deviation of successive differences. **pNN50** = percentage of the number of adjacent RR intervals which differ more than 50 ms. **meanRR** = arithmetic mean value of all RR intervals. * $p < 0.05$ and ** $p < 0.01$ compared to outside water condition.

In the sitting position during immersion, the SDNN significantly increased ($p = 0.012$) compared to outside the water. In contrast, SDNN only showed a slight increase in the supine position.

The RMSSD significantly increased ($p = 0.012$) in the sitting position from outside the water (36.03 ms) to immersed in water (76.33 ms). In the supine position during immersion, this measure only slightly increased with no significant change.

The SDSD measure was significantly lower ($p = 0.0022$) sitting outside the water (36.08 ms) compared to sitting immersed in water (76.46 ms). In the supine position, it did not differ significantly.

In the sitting position outside the water, the pNN50 showed a significant decrease ($p = 0.0022$) compared to the immersed condition. Outside the water, the pNN50 showed a value of 6.43% and during immersion 18.24%. In the supine position, the two conditions showed no significant difference (immersed 18.24%, outside the water 16.43%, respectively).

The meanRR in the sitting position was significantly higher ($p = 0.0022$) in the immersed condition with 969 ms (61.9 bpm) compared to outside the water with 801 ms (74.9 bpm). In the supine position, the meanRR showed also only a slight difference in the two conditions. outside the water 977 ms (61.4 bpm), during water immersion 1017 ms (59.0 bpm).

Overall, all time parameters showed a significant increase in the sitting position during water immersion compared to outside the water. In contrast, the values did not differ significantly in the supine position. While immersed, the measures showed only a slight increase.

4.3.2. Frequency Domain Parameters

The HRV features in the frequency domain are visualized in Figure 9a. The power spectral density in the VLF range showed an increase in the sitting position during water immersion (767.4 ms^2) compared to the position outside the water (590.8 ms^2), which was statistically not significant. However, in the supine position, the power spectral density was lower during the immersed condition than at the poolside. The VLF showed a value of 442.4 ms^2 in the water in contrast to outside the water with 523.8 ms^2.

(**a**)

(**b**)
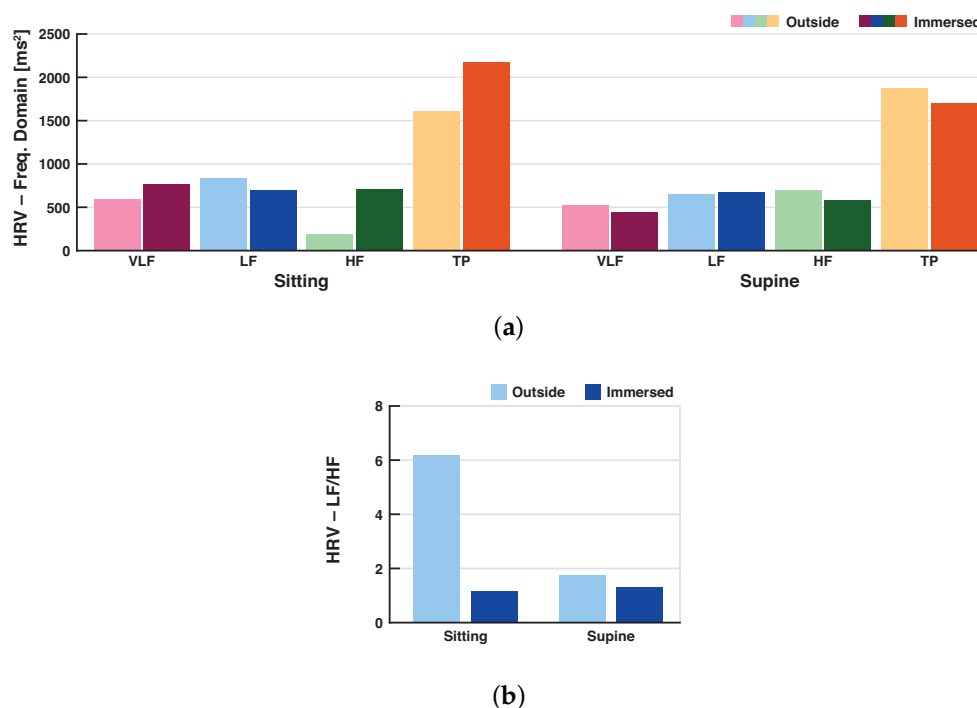
Figure 9. Frequency domain HRV parameters as a mean over all subjects. In (**a**), the changes in the very low frequency power (VLF), the low frequency (LF), and high frequency (HF) power as well as the total power (TP) are visualized between the outside-the-water (bright colors) and immersed condition (dark colors). On the left side of each subfigure the changes in the sitting position and on the right the changes in the supine position are given. In (**b**), the differences in the ratio LF/HF are visualized.

In the low-frequency range, the power density spectrum showed a different behavior compared to the very low-frequency range. With 831.6 ms^2 the measure for the LF range outside the water was increased compared to the immersed condition with 698.6 ms^2. In the supine position, both conditions, in and outside the water, did not differ significantly. The measurements at the poolside showed a LF of 654.6 ms^2, whereas during the immersed condition the value was 680.8 ms^2.

The power spectral density in the HF range was significantly decreased ($p = 0.0022$) during sitting outside the water in contrast to the water immersion. The HF value for the outside condition was

$188.5\,\text{ms}^2$, unlike during immersion $711.9\,\text{ms}^2$. In the supine position, this measure showed reverse behavior. Outside the water, the HF power spectral density was $699.4\,\text{ms}^2$ and in the water $583.7\,\text{ms}^2$.

Even the total power over all frequency ranges demonstrated such behavior in the VLF and the LF ranges. During sitting, the TP value was significantly lower ($p = 0.0022$) in the non-immersed condition ($1610\,\text{ms}^2$) compared to the measurements inside the water ($2178\,\text{ms}^2$). Also in the case of the power spectral density for the total power, a reverse characteristic in the supine position compared to the sitting position could be observed. During the immersion, the value was lower ($1707\,\text{ms}^2$) in contrast to the non-immersed condition ($1878\,\text{ms}^2$).

The ratio between the low-frequency and the high-frequency range (see Figure 9b) in the sitting position indicated a significantly higher value outside the water compared to immersion ($p = 0.0022$). The ratio between the LF and the HF range in the non-immersed sitting position was 6.20, during immersion 1.15. In the supine position, the differences were not that large. For the measurements at the poolside, the ratio was slightly higher with 1.76 compared to during the immersion with 1.32.

Table 2 shows a summary of the evaluated results as a mean over all subjects in the frequency domain.

Table 2. Frequency domain HRV parameters as a mean over all subjects.

Parameter	Sitting Outside Water	Sitting Inside Water	Supine Outside Water	Supine Inside Water
VLF [ms^2]	590.8	767.4	523.8	442.4
LF [ms^2]	831.6	698.6	654.6	680.8
HF [ms^2]	188.5	711.7 **	699.4	583.7
TP [ms^2]	1611	2178 **	1878	1707
LF/HF	6.20	1.15 **	1.76	1.32

VLF = very low-frequency power. **LF** = low-frequency power. **HF** = high-frequency power. **TP** = total power. **LF/HF** = ratio between LF and HF. ** $p < 0.01$ compared to outside water condition.

5. Discussion

In this work, an ECG sensor for underwater measurements was designed. Our previous current-based concept [18,19] was implemented and extended. Originally intended for the measurement of muscle activity in electromyograms, we showed that the concept works equally well for the measurement of the electrocardiogram in underwater conditions. In order to evaluate the new developed sensor during real applications, the sensor was tested in different conditions: outside and inside the water, as well as during rest and movements. The results of the small bandwidth configuration showed an almost noiseless signal quality, also under immersed conditions. Looking at the direct signal output of the ADC, we noticed a much higher signal amplitude of the R peak in the QRS complexes acquired by the current-based circuit when the electrodes and the subject were fully head-out immersed in water. We suspect that this is due to the high conductivity of the water surrounding the metal plate electrodes on the subject's body which increased the current flow into the electrode interface substantially. Looking at different placements of the measurement electrode of this monopolar recording system, we found different configurations to work very well, particularly with the measurement electrode placed directly above the heart on the chest-skin at the third intercostal space between the sternum and the midclavicular line (configuration II in Figure 4). At several placement configurations, we did not record the electrical heart activity in a noticeable magnitude; for example, if both the measurement and the ground electrode are placed on the abdomen on the left and right lateral sides, respectively. We assume this has to do with disturbances in the electrical field of the heart activity inside the body. In the scope of this work, we did not research this further.

Even though the QRS complexes can be clearly identified in the current-based ECG signal, it is not entirely understood how this method allows an evaluation of all the parameters defined for the standard ECG and in particular, for abnormality detection [28]. Since with our monopolar

system, only the entire summed-up electrical field of the heart (i.e., the changes in it) is measured, and not a particular directional derivation of it, it is not trivial to translate specific definitions of pathological electrical activity, seen in certain derivations of the potential ECG, to the current-based system. This needs further research.

The proposed current measurement technology was implemented into the FitnessSHIRT platform (electrical back-end) as introduced by the Frauenhofer IIS (Erlangen, Germany) [21]. However, we did not use, or test this to its full potential. The FitnessSHIRT platform's core element, the shirt itself with integrated tissue-based electrodes, could not be used in our study due to restrictions in the manufacturing process of the initial prototype circuit of the system. Furthermore, we decided that for prototype usage, it would be more suitable to have external electrode connectors available to allow for very similarly designed experiments between our circuit and Gold-standard reference sensors, which are also cable-based. In this way, we were able to ignore the influence of the entire cabling in both systems, as they had the same length and quality for all experiments. Also, the sensors (reference and current-based) could be held in the same locations (at the poolside).

One interesting finding in this regard is that the largest difference between the potential- and current-based systems can be seen when using metal-plate electrodes. Only in this case, the full distortion effect of the highly conductive water surrounding the electrodes is noticeable. When using highly adhesive, foam-based Ag/AgCl electrodes, there is not a large difference in signal quality between the two systems. This is likely due to the high shielding factor of the foam material and the much higher conductivity of the electrode gel between the skin and the electrode surface. As the electrodes are covered by the gel on the one side and the connector and foam on the other side, the signal degrades over time only when the water washes away the electrode gel and the conductivity of the water is lower than that of the gel. We also did not evaluate how a high saline content of water would change the outcome of our physiological measurements. We do not expect different outcomes when using metal-plate electrodes, however, for gel-based adhesive electrodes it might make a difference.

The results of the heart rate variability study endorse the physiological response to immersion showing an initial reflex bradycardia resulting from a restriction of blood flow to the peripheries and to venoconstriction due to hydrostatic forces, typically known as the mammalian diving reflex [29]. In general, immersion results in an increase of venous return, increased stroke volume and bradycardia as a modest increase in cardiac output [30]. It is expected that the effect of the mammalian diving reflex is amplified during full immersed conditions, since a high density of baro- and temperature receptors is located in the face. However, since it was not the direct aim of the HRV study to investigate the particular changes of the heart activity between submerged conditions, we do not discuss this further. This has already been the topic of various previous research. For example, Flouris et al. evaluated the HRV changes during a challenging dive [31], Kinoshita et al. during face submersion in cold water [32], Kiviniemi et al. during static and dynamic breath-hold dives [33] or Perini et al. during exercises inside and outside the water [34]. Instead, the primary goal of this study, in the context of our developed sensor, was to demonstrate its applicability for such endeavors. We were successfully able to reproduce the characteristics in the HRV in dry and submerged conditions as reported by previous studies with potential-based ECG sensors [4]. This allows us to assume that our sensor can be used to perform accurate and repeatable measurements of the human ECG in dry and underwater conditions for physiological experiments or monitoring, in particular for the important evaluation of the HRV.

6. Conclusions

In this work, we designed an ECG sensor for underwater measurements to gain insights into cardiac activity during immersion. We showed that the transimpedance amplifier-based circuit design not only works in dry conditions for the measurement of the human ECG, but also underwater. We were able to successfully reproduce the most important changes in HRV seen between dry and immersed conditions [4]. With the significant changes in SDSD, pNN50, meanRR, HF, TP and consequently

LF/HF, we clearly show that our system measures a clear ECG signal underwater that allows precise extraction of RR-intervals. Interestingly, in an immersed condition, signals from the electrical heart activity were registered with a higher signal amplitude than in the dry condition. We provided some ideas for the cause of this and will research this further. In the future, we also plan to investigate the system behavior in deeper water with fully immersed subjects, including different placements of the measurement electrodes on the body, ideally allowing the extraction of a body mapping for currents, similar to the body surface potential maps [35]. In the current study, we verified that our system is capable of measuring at depths up to 1.5 m with full body immersion; however, we did not evaluate this further. The next step is to make the circuit board housing watertight for up to 50 m and perform additional diving experiments in the open sea with larger water currents and high saline levels of the water. We are also presently working on a bipolar version of this current-based circuit to allow directional derivations of the electrical field changes. Furthermore, we want to investigate the electrical properties of the skin–electrode interface of this circuit design in more detail.

The newly developed ECG sensor represents a platform to fundamentally investigate and evaluate cardiac activities in immersed conditions with the potential of having a major impact in both engineering and medical research. On the one hand, engineering research may focus on the full disclosure of the transimpedance amplifier compared to commercial instrumental amplifiers and their differences in spatial resolution and the suppression of noises and artifacts. On the other hand, medical research may focus on the investigation of cardiac diseases and physiological occurrences triggered underwater, achieved by measurements obtained using the presented current-based technology.

Author Contributions: Stefan Gradl, Vinzenz von Tscharner, and Bjoern M. Eskofier conceived and designed the experiments; Vinzenz von Tscharner, Jasmine Lauber, and Ruslan Rybalko designed and built the circuit and other connected hardware components; Stefan Gradl, Jasmine Lauber, and Tobias Cibis performed the experiments and analyzed the data; Stefan Gradl, Tobias Cibis, Robert Richer, Norman Pfeiffer, Heike Leutheuser, Markus Wirth, Vinzenz von Tscharner, and Bjoern M. Eskofier wrote the paper.

Conflicts of Interest: The authors declare no conflict of interest.

References

1. Buzzacott, P. *Dan Annual Diving Report*; Divers Alert Network: Durham, NC, USA, 2015.
2. Bennett, M. Cardiac Problems and Sudden Death. In *Diving and Subaquatic Medicine*, 5th ed.; Edmonds, C., Bennett, M., Lippmann, J., Mitchell, S., Eds.; CRC Press: Boca Raton, FL, USA, 2015; pp. 449–457.
3. Malik, M.; Bigger, J.T.; Camm, A.J.; Kleiger, R.E.; Malliani, A.; Moss, A.J.; Schwartz, P.J. Heart Rate Variability: Standards of Measurement, Physiological Interpretation and Clinical Use. Task Force of the European Society of Cardiology and the North American Society of Pacing and Electrophysiology. *Circulation* **1996**, *93*, 1043–1065.
4. Schipke, J.D.; Pelzer, M. Effect of Immersion, Submersion, and Scuba Diving on Heart Rate Variability. *Br. J. Sport Med.* **2001**, *35*, 174–180.
5. Salahuddin, L.; Cho, J.; Jeong, M.G.; Kim, D. Ultra Short Term Analysis of Heart Rate Variability for Monitoring Mental Stress in Mobile Settings. In Proceedings of the Annual International Conference of the IEEE Engineering in Medicine and Biology Society, Lyon, France, 22–26 August 2007; Volume 2007, pp. 4656–4659.
6. Myers, G.A.; Martin, G.J.; Magid, N.M.; Barnett, P.S.; Schaad, J.W.; Weiss, J.S.; Lesch, M.; Singer, D.H. Power Spectral Analysis of Heart Rate Varability in Sudden Cardiac Death: Comparison to Other Methods. *IEEE Trans. Biomed. Eng.* **1986**, *33*, 1149–1156.
7. Richer, R.; Groh, B.H.; Blank, P.; Dorschky, E.; Martindale, C.; Klucken, J.; Eskofier, B.M. Unobtrusive Real-Time Heart Rate Variability Analysis for the Detection of Orthostatic Dysregulation. In Proceedings of the IEEE

13th International Conference on Wearable and Implantable Body Sensor Networks (BSN), San Francisco, CA, USA, 14–17 June 2016.

8. Cibis, T.; McEwan, A.; Eskofier, B.; Lippmann, J.; Friedl, K.; Bennett, M. Diving into Research of Biomedical Engineering in Scuba Diving. *IEEE Rev. Biomed. Eng.* **2017**, doi:10.1109/RBME.2017.2713300.

9. Baig, M.M.; Gholamhosseini, H.; Connolly, M.J. A Comprehensive Survey of Wearable and Wireless Ecg Monitoring Systems for Older Adults. *Med. Biol. Eng. Comput.* **2013**, *51*, 485–495.

10. Bosco, G.; De Marzi, E.; Michieli, P.; Omar, H.R.; Camporesi, E.M.; Padulo, J.; Paoli, A.; Mangar, D.; Schiavon, M. 12-Lead Holter Monitoring in Diving and Water Sports: A Preliminary Investigation. *Diving Hyperb. Med.* **2014**, *44*, 202–207.

11. Cibis, T.; Groh, B.H.; Gatermann, H.; Leutheuser, H.; Eskofier, B.M. Wearable Real-Time Ecg Monitoring with Emergency Alert System for Scuba Diving. In Proceedings of the 37th Annual International Conference of the IEEE Engineering in Medicine and Biology Society (EMBC), Milan, Italy, 25–29 August 2015; pp. 6074–6077.

12. Gradl, S.; Kugler, P.; Lohmüller, C.; Eskofier, B. Real-Time Ecg Monitoring and Arrhythmia Detection Using Android-Based Mobile Devices. *Conf. Proc. IEEE Eng. Med. Biol. Soc.* **2012**, 2452–2455, doi:10.1109/EMBC.2012.6346460.

13. Barrett, P.M.; Komatireddy, R.; Haaser, S.; Topol, S.; Sheard, J.; Encinas, J.; Fought, A.J.; Topol, E.J. Comparison of 24-Hour Holter Monitoring with 14-Day Novel Adhesive Patch Electrocardiographic Monitoring. *Am. J. Med.* **2014**, *127*, doi:10.1016/j.amjmed.2013.10.003.

14. Ohtsu, M.; Fukuoka, Y.; Ueno, A. Underwater Electromyographic Measurement Using a Waterproof Insulated Electrode. *Adv. Biomed. Eng.* **2012**, *1*, 81–88.

15. Reyes, B.A.; Posada-Quintero, H.F.; Bales, J.R.; Clement, A.L.; Pins, G.D.; Swiston, A.; Riistama, J.; Florian, J.P.; Shykoff, B.; Qin, M. Novel Electrodes for Underwater Ecg Monitoring. *IEEE Trans. Biomed. Eng.* **2014**, *61*, 1863–1876.

16. Reyes, B. Performance Evaluation of Carbon Black Based Electrodes for Underwater Ecg Monitoring. In Proceedings of the 36th Annual International Conference of the IEEE Engineering in Medicine and Biology Society (EMBC), Chicago, IL, USA, 26–30 August 2014.

17. Noh, Y.; Bales, J.R.; Reyes, B.A.; Molignano, J.; Clement, A.L.; Pins, G.D.; Florian, J.P.; Chon, K.H. Novel Conductive Carbon Black and Polydimethlysiloxane Ecg Electrode: A Comparison with Commercial Electrodes in Fresh, Chlorinated, and Salt Water. *Ann. Biomed. Eng.* **2016**, *44*, 2464–2479.

18. Von Tscharner, V.; Maurer, C.; Ruf, F.; Nigg, B.M. Comparison of Electromyographic Signals from Monopolar Current and Potential Amplifiers Derived from a Penniform Muscle, the Gastrocnemius Medialis. *J. Electromyogr. Kinesiol.* **2013**, *23*, 1044–1051.

19. Whitting, J.W.; von Tscharner, V. Monopolar Electromyographic Signals Recorded by a Current Amplifier in Air and under Water without Insulation. *J. Electromyogr. Kinesiol.* **2014**, *24*, 848–854.

20. Inan, O.T.; Kovacs, G.T. An 11 Mu W, Two-Electrode Transimpedance Biosignal Amplifier with Active Current Feedback Stabilization. *IEEE Trans. Biomed. Circuits Syst.* **2010**, *4*, 93–100.

21. Leutheuser, H.; Lang, N.R.; Gradl, S.; Struck, M.; Tobola, A.; Hofmann, C.; Anneken, L.; Eskofier, B.M. Textile Integrated Wearable Technologies for Sports and Medical Applications. In *Smart Textiles*; Springer: Berlin, Germany, 2017; pp. 359–382.

22. Thakor, N.V.; Webster, J.G.; Tompkins, W.J. Estimation of Qrs Complex Power Spectra for Design of a Qrs Filter. *IEEE Trans. Biomed. Eng.* **1984**, *31*, 702–706.

23. Kwatra, S.C.; Jain, V.K. A New Technique for Monitoring Heart Signals-Part I: Instrumentation Design. *IEEE Trans. Biomed. Eng.* **1986**, *BME-33*, 35–41.

24. Wittling, W.; Wittling, R.A. *Herzschlagvariabilität: Frühwarnsystem, Stress-Und Fitnessindikator: Grundlagen—Messmethoden—Anwendungen*; Eichsfeld-Verlag: Heilbad Heiligenstadt, Germany, 2012.

25. Elgendi, M. Fast Qrs Detection with an Optimized Knowledge-Based Method: Evaluation on 11 Standard Ecg Databases. *PLoS ONE* **2013**, *8*, doi:10.1371/journal.pone.0073557 .

26. Gradl, S.; Leutheuser, H.; Elgendi, M.; Lang, N.; Eskofier, B.M. Temporal Correction of Detected R-Peaks in Ecg Signals: A Crucial Step to Improve Qrs Detection Algorithms. *Conf. Proc. IEEE Eng. Med. Biol. Soc.* **2015**, 522–525, doi:10.1109/EMBC.2015.7318414.

27. Shaffer, F.; Ginsberg, J.P. An Overview of Heart Rate Variability Metrics and Norms. *Front. Public Health* **2017**, *5*, doi:10.3389/fpubh.2017.00258.

28. Prineas, R.J.; Crow, R.S.; Zhang, Z.M. *The Minnesota Code Manual of Electrocardiographic Findings*; Springer Science & Business Media: Berlin, Germany, 2009.

29. Brubakk, A.; Neuman, T.S. *Bennett and Elliotts' Physiology and Medicine of Diving*, 5th ed.; W.B. Saunders: Amsterdam, The Netherlands, 2006.

30. Boussuges, A.; Blanc, F.; Carturan, D. Hemodynamic Changes Induced by Recreational Scuba Diving. *CHEST J.* **2006**, *129*, 1337–1343.

31. Flouris, A.D.; Scott, J.M. Heart Rate Variability Responses to a Psychologically Challenging Scuba Dive. *J. Sports Med. Phys. Fit.* **2009**, *49*, 382–386.

32. Kinoshita, T.; Nagata, S.; Baba, R.; Kohmoto, T.; Iwagaki, S. Cold-Water Face Immersion Per Se Elicits Cardiac Parasympathetic Activity. *Circ. J.* **2006**, *70*, 773–776.

33. Kiviniemi, A.M.; Breskovic, T.; Uglesic, L.; Kuch, B.; Maslov, P.Z.; Sieber, A.; Seppanen, T.; Tulppo, M.P.; Dujic, Z. Heart Rate Variability During Static and Dynamic Breath-Hold Dives in Elite Divers. *Auton. Neurosci.* **2012**, *169*, 95–101.

34. Perini, R.; Milesi, S.; Biancardi, L.; Pendergast, D.R.; Veicsteinas, A. Heart Rate Variability in Exercising Humans: Effect of Water Immersion. *Eur. J. Appl. Physiol.* **1998**, *77*, 326–332.

35. Kornreich, F.; Rautaharju, P.M.; Warren, J.; Montague, T.J.; Horacek, B. Multigroup Diagnosis of Body Surface Potential Maps. *Am. J. Cardiol.* **1985**, *56*, 169–178.